Published in final edited form as:
J Med Chem. 2010 September 23; 53(18): 6747–6757. doi:10.1021/jm100592u.

Design, Synthesis, and Evaluation of 1,4,7,10-Tetraazacyclododecane-1,4,7-triacetic Acid-Derived, Redox-Sensitive Contrast Agents for Magnetic Resonance Imaging

Natarajan Raghunand[†], **Gerald P. Guntle**[¶], **Vijay Gokhale**[‡], **Gary S. Nichol**[§], **Eugene A. Mash**[§], and **Bhumasamudram Jagadish**[*,§]

[†]Department of Radiology, University of Arizona, Tucson AZ 85724-5024

[¶]Cancer Center Division, University of Arizona, Tucson AZ 85724-5024

[‡]Department of Pharmacology and Toxicology, University of Arizona, Tucson, AZ 85721-0240

[§]Department of Chemistry and Biochemistry, University of Arizona, Tucson, AZ 85721-0041

Abstract

The design and synthesis of three 1,4,7,10-tetraazacyclododecane-1,4,7-triacetic acid (DO3A) derivatives bearing linkers with terminal thiol groups and a preliminary evaluation of their potential for use in assembling redox-sensitive Magnetic Resonance Imaging (MRI) contrast agents are reported. The linkers were selected based on computational docking with a crystal structure of human serum albumin (HSA). Gd(III)-DO3A and Eu(III)-DO3A complexes were synthesized, and the structure of one complex was established by X-ray crystallographic analysis. The binding to HSA of a Gd(III)-DO3A complex bearing a thiol-terminated 3,6-dioxanonyl chain was competitively inhibited by homocysteine and by the corresponding Eu chelate. Binding to HSA was abolished when the terminal thiol group of this complex was absent. The longitudinal water-proton relaxivities (r_1) of the three Gd(III)-DO3A complexes and of two Gd(III)-1,4,7,10-tetraazacyclododecane-1,4,7,10-tetraacetic acid (DOTA) complexes were measured in saline at 7 Tesla. The DO3A complexes exhibited smaller r_1 values, in both bound and free states, than the DOTA complexes.

Introduction

Advances in our understanding of the molecular pathogenesis of cancer and many other diseases have lead to the current push toward the development of novel, targeted drugs. This is being accompanied by a transformation of diagnostic radiology from a discipline focused on the imaging of anatomy to one that seeks to interrogate tissue physiology and molecular phenotypes, and provide non-invasive imaging biomarkers of drug targets and drug action. Magnetic Resonance Imaging (MRI)a is a powerful medical diagnostic tool, and while not

[*]Address correspondence to Dr. Bhumasamudram Jagadish, Department of Chemistry and Biochemistry, University of Arizona, 1306 East University, P.O. Box 210041, Tucson, AZ 85721-0041 USA; Phone (520) 621-2396; FAX (520) 621-8407; bjagadis@email.arizona.edu.

Supporting Information Available. General experimental procedures, proton and carbon NMR spectra for compounds **3b–5b, 8, 11, 13, 17, 19a–c, 20a–c**, and **21–23**, mass spectra for compounds **3a–5a, 3b–5b**, and **24**, and an X-ray crystallographic information file (CIF) for compound **4a**. This material is available free of charge via the Internet at http://pubs.acs.org

[a]Abbreviations: ARE, antioxidant response element; CAs, contrast agents; DCM, dichloromethane; DO3A, 1,4,7,10-tetraazacyclododecane-1,4,7-triacetic acid; DOTA, 1,4,7,10-tetraazacyclododecane-1,4,7,10-tetraacetic acid; HEPES, 4-(2-hydroxyethyl)-1-piperazineethanesulfonic acid; HSA, human serum albumin; GGT, γ-glutamyltransferase; MRI, magnetic resonance imaging; MRP, multidrug resistance-associated protein; PBS, phosphate buffered saline; PEG, polyethylene glycol; TBAI, tetrabutylammonium iodide.

all MRI examinations require the administration of exogenous contrast material, in clinical practice many MRI examinations employ gadolinium(III)-based contrast agents (CAs).[1–3] The efficacy of an MRI contrast agent is dependent on its relaxivity, and in the last two decades much work has been devoted to understanding the parameters that influence the relaxation properties of these CAs.[4–6] Clinically approved MRI CAs are suited primarily for highlighting anatomical features on MR images, after intravenous administration and vascular distribution throughout the body. In recent years, the focus has shifted towards the development of MRI CAs that are sensitive to physiochemical changes and biochemical changes in their microenvironment, such as pH, pO_2, metal ion concentration, enzymatic activity, and redox state.[7–21] Perturbations of tissue redox are linked to the development of hyperglycemia-induced vascular and renal complications in diabetes mellitus.[22,23] Evidence also suggests that altered redox homeostasis in cancer cells plays a role in tumor progression and metastasis,[24–26] chemoresistance,[25] and radioresistance.[27] The Nrf2 transcription factor, which is upregulated in many cancers,[26] transcriptionally upregulates antioxidant response element (ARE)-containing genes. ARE-containing genes include many that impinge on tissue levels of reduced glutathione, thioredoxin, and cysteine, and code for drug transporters such as the multidrug resistance-associated protein (MRP).[25] Reduced thiols such as glutathione and cysteine can directly effect the chemical repair of DNA damage produced by ionizing radiation, thereby providing a degree of radioprotection.[28] Nrf2-regulated γ-glutamyltransferase (GGT) can modulate redox equilibria in both the intracellular and extracellular compartments.[29,30] GGT can confer a degree of protection to cancer cells from electrophilic drugs such as cisplatin by increasing the extracellular levels of thiols.[29,30] Knowledge of tumor redox by itself, and knowledge of tumor redox as a potential downstream biomarker of tumor Nrf2 status, is thus greatly relevant to the management and treatment of cancer. We report the development of thiol-sensitive MRI contrast agents for potential use in the non-invasive interrogation of tumor redox.

Previously we reported the synthesis and characterization of compounds **1** and **2**, 1,4,7,10-tetraazacyclododecane-1,4,7,10-tetraacetic acid (DOTA) complexes of gadolinium(III) bearing alkyl chains that terminate with a thiol group.[31] These compounds bound to human serum albumin (HSA) in a redox-sensitive manner, as evidenced by increased MRI relaxivity and retention in a 30 kDa MWCO filter in the presence of HSA. Loss of both these properties occurred when **1** and **2** were competed with excess homocysteine, which is known to form a disulfide link with cysteine-34 of HSA. More recently, Lacerda, et al., prepared a 1,4,7,10-tetraazacyclododecane-1,4,7-triacetic acid (DO3A) macrocycle bearing a terminal β-thioethyl appendage for use as a chelating agent for radionuclides.[32] The synthesis of glyconanoparticles capped with a Gd-DO3A chelate bearing pentyl and undecyl appendages with terminal thiol groups has also been reported.[33] In a continuation of our work, we have designed and synthesized three DO3A chelators bearing different types of linkers that terminate with thiol groups, prepared the corresponding Gd and Eu complexes **3–5**, obtained a crystal structure of Gd-DO3A complex **4a**, studied the binding of these complexes to HSA, and have evaluated the relaxivity of these complexes in the presence and absence of HSA as reported herein.

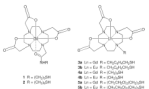

Molecular modeling of the interactions between compounds 1–5 and HSA

We postulated that compounds such as **1–5** may bind to HSA via one or more of the following: formation of a covalent disulfide bond between the thiol-terminated linker and the Cys34–SH group, linker-protein interactions, and interactions between the chelate

moiety and a hydrophobic pocket near the surface of the protein. Our current modeling effort employs a known X-ray crystal structure of HSA34 to design molecules that will maximize binding based on these three key interactions. Figure 1 shows a possible binding site located on the surface of HSA near Cys34. The site consists of a hydrophobic binding pocket and a hydrophobic channel leading from the pocket to Cys34. The pocket is formed by Gly82, Thr83, Tyr84 (backbone), Gly85, Glu86, and Met87 on one side and by Gln104, His105, Lys106, Asp107, Asp108, Glu465, Lys466, and Thr467 on the other side. These residues create a bowl-shaped depression where the chelate moiety might nest. The backbone and side chains of Tyr30, Leu31, Gln32, Gln33, and Tyr84 create a hydrophobic channel where an appropriate linker might bind while permitting covalent attachment of a terminal thiol to the Cys34–SH group.

Our molecular modeling protocol was designed to simulate a possible two stage binding process.35 In the first stage, non-covalent interactions between compounds **1–5** and the putative binding site described above were computationally examined in the presence of water molecules. During these simulations, movement of the protein side chains to accommodate small molecule docking was allowed. In the second stage, a covalent disulfide linkage between the terminal thiol of the small molecule and the Cys34–SH was established, and the simulations were repeated. At the end of each docking simulation, the interaction energy value was calculated.

For the DOTA-containing compounds **1** and **2**, Gd chelation by the amide group in the linker provides an extra measure of structural rigidity. Covalent binding of **2** to HSA results in additional coordination by the backbone C=O groups of Thr83 or Tyr84 and one water molecule (see Figure 2). It is hypothesized that the system is dynamic, and that Thr83, Tyr84, and water exchange in the coordination sphere of the gadolinium atom. Compound **2** exhibited a greater interaction energy (−510 kcal/mol, see Table 1) than did **1** (−290 kcal/mol), presumably due to increased van der Waals interactions with the channel. These calculations were qualitatively consistent with the measured binding constants of **1** and **2** (see Table 1).

In contrast with Gd-DOTA chelates in which only one water molecule may be coordinated with the Gd (q = 1), Gd-DO3A chelates allow for the possibility of two coordinated water molecules (q = 2) and may exhibit very different binding to HSA and different MRI relaxivity characteristics. In modeling Gd-DO3A chelates, the three linkers shown in compounds **3–5** were selected from a number of possibilities that were initially considered. Included are linkers based on a rigid hydrophobic *p*-xylyl group, a flexible hydrophobic nonyl chain, and a flexible hydrophilic 3,6-dioxanonyl chain. Figure 3 shows an overlay of energy-minimized structures for compounds **3a–5a**.

In the computational docking studies, compound **3a** possessing the xylyl linker exhibited somewhat weaker binding (−410 kcal/mol, see Table 1) than did compounds **4a** and **5a** (−471 and −453 kcal/mol, respectively). The xylyl linker has neither the reach nor the flexibility of the nonyl and 3,6-dioxanonyl chains which are able to interact more favorably with the channel connecting Cys34 and the hydrophobic binding pocket on the surface of HSA. Still, docking indicates that all the three compounds show similar profiles with respect to binding of the gadolinium chelate moiety. Backbone amide C=O groups of Thr83 and Tyr84 and one water molecule are in the inner coordination sphere of the gadolinium atom (Table 1). In simulations carried out in water, two water molecules occupy two inner sphere coordination sites for each of the DO3A chelates **3a–5a**. Thus, one would expect different relaxivity for protein-bound and unbound chelates, and so these compounds were selected for synthesis and evaluation of binding and relaxivity properties.

Synthesis

A retrosynthetic analysis for construction of Ln-DO3A conjugates **3–5** is depicted in Scheme 1. A key step would be the simultaneous deprotection of the three *tert*-butyl esters and the tritylthio group in **7** to afford DO3A derivatives **6**, which, upon complexation with the desired lanthanide, would give the complexes **3–5**. *N*-Alkylation of the known DO3A derivative **8** with primary bromides **9** would give access to **7**.

The required bromides were synthesized as shown in Scheme 2. Bromide **11**36 was prepared by reacting *p*-xylene dibromide **10** with trityl mercaptan and sodium hydride in anhydrous THF. Bromide **13** was similarly prepared by reacting 1,9-dibromononane (**12**) with trityl mercaptan and K_2CO_3 in acetonitrile. Bromide **17** was prepared in three steps. 1,3-Dibromopropane (**14**) was reacted with trityl mercaptan and K_2CO_3 in acetonitrile to give **15**. Bromide **15** was converted to **16** by reaction with diethylene glycol, sodium hydride, and TBAI in dry THF.37 Finally, bromination of **16** with CBr_4 and PPh_3 gave **17**.38

Ester **8** was prepared from commercially available cyclen **18** by treatment with 3 equivalents of *tert*-butyl bromoacetate and sodium acetate in *N,N*-dimethylacetamide using a modification of a published procedure (Scheme 3).39 *N*-Alkylation of **8** with bromide **11** in acetonitrile using K_2CO_3 as base gave **19a** in 80% yield. Simultaneous removal of *tert*-butyl and trityl groups was attempted by treatment of **19a** with triethylsilane and trifluoroacetic acid (1% v/v). Under these conditions, it appeared that the trityl group came off easily, while the ester groups were incompletely hydrolyzed. Longer reaction times and the use of solvents such as dichloromethane and chloroform led to what appeared by mass spectrometry to be the monoester derivative.40 We reasoned that this was not a case of incomplete ester hydrolysis, but rather of capture of a *tert*-butyl cation by the thiol group after loss of the trityl group. To eliminate this undesired process, an excess of butanethiol was added to the reaction medium to scavenge *tert*-butyl cations. This led to isolation of the fully deprotected tricarboxylic acid **20a** in 80% yield. Acid **20a** was metalated with $Gd(OAc)_3$ or $Eu(OAc)_3$ in refluxing methanol to give the corresponding Gd(III) and Eu(III) complexes **3a** and **3b** in 75% and 71% yields, respectively, following reverse phase silica gel chromatography.

Following a similar synthetic pathway, amine **8** was alkylated with bromide **13** to give **19b** in 80% yield. Deprotection of **19b** produced **20b** in 75% yield, and metalation of **20b** with $Gd(OAc)_3$ and $Eu(OAc)_3$ in refluxing methanol gave the complexes **4a** and **4b** in 57% and 58% yields, respectively, following reverse phase silica gel chromatography. Finally, *N*-Alkylation of **8** with **17** gave **19c** in 92% yield. Deprotection of **19c** gave **20c** in 75% yield, and metalation of **20c** with $Gd(OAc)_3$ and $Eu(OAc)_3$ produced complexes **5a** and **5b** in 75% and 82% yields, respectively, following reverse phase silica gel chromatography.

In addition to the syntheses of **3a–5a** and **3b–5b**, the synthesis of Gd-DO3A complex **24** is depicted in Scheme 4. Bromide **21** was prepared from diethylene glycol monopropyl ether in 90% yield by use of the Appel reaction.38 Alkylation of **8** with **21** in acetonitrile using K_2CO_3 as base gave **22** in 87% yield. Deprotection of the *t*-butyl ester groups using TFA in DCM gave tricarboxylic acid **23** in 77% yield. Metalation with $Gd(OAc)_3$ hydrate in refluxing methanol gave complex **24** in 75% yield following reverse phase silica gel chromatography.

The structures of all compounds, except **3a, 4a, 5a**, and **24**, were characterized by ^1H NMR, ^{13}C NMR, and HRMS. Compounds **3a–5a, 3b–5b**, and **24** gave appropriate masses and isotopic patterns in HRMS analysis (see the Supporting Information). Further evidence for the structures of the Gd-DO3A macrocycles was obtained by X-ray crystallographic analysis of **4a**. Crystals were grown according to a procedure used previously for growing

an In-DO3A–TPP complex.41 An equimolar mixture of **20b** and $Gd(OAc)_3$ was heated at 100°C for 30 min in NH_4OAc buffer (0.5 M, pH = 6). Slow diffusion of acetone into the reaction mixture produced colorless, flat plates. Compound **4a** crystallized in space group *P*-1 as a dihydrate with an acetate anion coordinated to the gadolinium center (Figure 5) and a charge-balancing ammonium cation present in the asymmetric unit. Water is also present in the asymmetric unit, some of which was removed by SQUEEZE.42 There is some disorder in the ω-thiononyl chain, which adopts a mostly extended conformation.43

Binding and Relaxometry

The binding of compounds **1, 2, 3a–5a**, and **24** to commercially obtained HSA was measured at 37°C in buffered saline (see Table 1). For commercial samples, some percentage of the HSA present bears homocysteine or another thiol of low molecular weight covalently attached at Cys34.44 Thus, calculation of an apparent equilibrium association constant (K_A) was possible from the binding experiments described herein. Compounds **3a** and **4a** bound to HSA with a stoichiometry >3:1 (data not shown), while compounds **1, 2**, and **5a** bound to HSA with a stoichiometry ~1:1. For compound **5a**, $K_A = 22\ mM^{-1}$, a value intermediate between the published values for DOTA complexes **1** and **2**.31 The binding of compounds **1, 2**, and **5a** to HSA could be competitively inhibited by addition of homocysteine (see Table 2). The binding of **5a** to HSA was inhibited even more effectively by the structurally related Eu chelate, **5b**. Binding to HSA was abolished for **24**, a compound similar to **5a** but lacking the terminal thiol group.

The longitudinal water-proton relaxivities (r_1) of compounds **1, 2**, and **5a** were measured in HEPES-buffered saline. For compounds **3a** and **4a**, r_1 was measured in acetate-buffered saline because these complexes were poorly soluble in the absence of acetate. Results reported include r_1(free), determined in the absence of HSA, and r_1(bound), determined in the presence of this protein (see Table 3). The DO3A–based complexes had smaller relaxivities, in both bound and free states, than the DOTA-based complexes. For compounds **1, 2, 4a**, and **5a**, r_1(free) was smaller than r_1(bound), most likely due to increased times for rotational reorientation of the complexes when bound to HSA. In the case of **3a**, r_1(free) was comparable to values observed for the other DO3A chelates, **4a** and **5a**, but r_1(bound) was smaller than r_1(free), suggesting that other factors limit the relaxivity of **3a** when bound to HSA.

Discussion

Calculated interaction energies for compounds **1, 2, 3a–5a**, and **24** with HSA are given in Table 1. The covalent interaction energies, which include a disulfide linkage, are lower (i.e., the covalent complex is more stable) than the corresponding noncovalent interaction energies. The differences in the calculated covalent and noncovalent interaction energies are 80, 14, 44, 67, and 40 kcal/mol for compounds **1, 2**, and **3a–5a**, respectively, in reasonable agreement with typical disulfide bond strengths (70 kcal/mol).45 In the case of compound **2**, the energy gained through disulfide bond formation is presumably counterbalanced by losses of other stabilizing interactions. Consistent with this interpretation, the calculated noncovalent interaction energies for **5a** and compound **24**, which lacks a terminal thiol group and cannot form a disulfide bond, are very similar. In addition, the calculated covalent interaction energies correlate reasonably well with experimentally determined apparent equilibrium binding constants (K_A, Table 1).

Homocysteine is known to bond covalently with Cys34 of HSA.44 Increasing concentrations of homocysteine resulted in corresponding decreases in K_A for compounds **1, 2**, and **5a** (see Table 2), suggesting that these compounds also bond with HSA at Cys34. In

contrast, compounds **3a** and **4a** exhibited essentially complete and irreversible binding to HSA. Due to insolubility, binding assays for these compounds were carried out in acetate-buffered saline. In the centrifugal filtration assay used to quantify binding, essentially no Gd was recovered in the filtrates from incubations of up to 2.0 mM **3a** or **4a** with 0.66 mM HSA (3:1). These results were unchanged when up to 2.0 mM homocysteine was included, indicating that **3a** and **4a** bind to HSA at sites other than Cys34. In aqueous solutions **3a** and **4a** would be expected to possess two water molecules in the inner coordination sphere (see Table 1).46 Displacement of inner sphere water molecules by acetate is a possible reason why the r_1(free) values for **3a** and **4a** are lower than those of the DOTA complexes, **1** and **2**. In addition, it has been reported that inner sphere water molecules can be displaced by carboxylate groups on albumin.47 There are 97 aspartate and glutamate residues in HSA. Examination of the X-ray crystal structure suggests that the majority of side chain carboxylate groups are present on the protein surface. Given the low solubility of **3a** and **4a** in the absence of acetate and the presence of a bifurcated acetate ligand in the crystal structure of **4a**, it is conceivable that carboxylate groups on the HSA surface constitute the multiple sites to which these compounds bind. Displacement of inner sphere water molecules would also help explain the surprisingly low value of r_1(bound) observed for **3a**. Compound **5a** might possess only one water molecule in the inner coordination sphere since the oxygen atom in the PEG sidechain proximal to the DO3A moiety can coordinate to gadolinium.48 Thus, **5a** might exhibit properties more like those of a DOTA complex. However, r_1(free) and r_1(bound) for **5a** were significantly lower than values for **1** and **2**, possibly due to suboptimal coordination geometry or decreased basicity of the macrocyclic nitrogen that bears the pendant arm.49

Conclusion

A general method for the synthesis of DO3A–based lanthanum chelates possessing different nitrogen-attached sidearms that terminate with redox-active thiol groups has been demonstrated. The synthesis is relatively short and efficient. To the best of our knowledge, the first X-ray crystal structure of a gadolinium-DO3A complex has been obtained. Taken together with protein binding and relaxivity data, the crystal structure supports the suggestion that coordination by surface carboxylate groups may be important in protein binding and water relaxivity for DO3A chelates *in vivo*.47 Direct and competition binding assays indicate that, for DOTA chelates and DOTA-like DO3A chelates bearing terminal thiol groups, covalent attachment through a disulfide linkage with Cys34 is an important mode of HSA binding. Studies to further examine the redox chemistry of gadolinium DO3A and DOTA chelates and the associated MRI properties are underway.

Experimental

Small molecule docking with HSA

An X-ray crystal structure of HSA (PDB code: 1AO6) was refined and used as the basis for docking simulations that were carried out using Insight II 2005L.35 Compounds to be docked were placed in the vicinity of the Cys34–SH group and the protein–small molecule system surrounded with a 7.5 Å layer of water. Charges were assigned using extensible systematic force field (ESFF).50 The gadolinium atom was assigned a +3.0 formal charge. The system was then energy minimized using 5000 steps, followed by a molecular dynamics simulation with a 50 picosecond equilibration and a 100 picosecond simulation at 300 K. Frames were collected after every 100 femtoseconds during the 100 picosecond simulation phase. At the end of the molecular dynamics run, trajectories were analyzed on the basis of potential energy. The frame with the lowest potential energy was further minimized using 5000 steps. During covalent simulations, an S-S linkage was first established between the thiol groups of the small molecule and Cys34. This was then followed by energy

minimization and molecular dynamics protocols as described above. Interaction energies were calculated as the difference between the energy of the small molecule-protein complex and the sum of the individual energies of the protein and the small molecule.

$$E_{interaction} = E_{complex} - (E_{small\ molecule} + E_{protein})$$

Simulations in aqueous solution

The small molecule of interest was surrounded with a 7.5 Å layer of TIP3P water molecules. The system was then minimized using 5000 steps. This was followed by a molecular dynamics simulation with a 50 picosecond equilibration and a 100 picosecond simulation at 300 K. Frames were collected after every 100 femtoseconds during the 100 picosecond simulation phase. At the end of the molecular dynamics run, trajectories were analyzed on the basis of potential energy. The frame with the lowest potential energy was further minimized using 5000 steps. This minimized frame was used to study the coordination of the gadolinium atom by water molecules.

Synthesis51

1-Bromomethyl-4-(triphenylmethylthio)methylbenzene (11).36—To a suspension of NaH (46 mg, 1.89 mmol) in dry THF (10 mL) was added a solution of trityl mercaptan (523 mg, 1.89 mmol) in dry THF (10 mL) with stirring. After 0.5 h, the solution was added dropwise to a solution of **10** (1.0 g, 3.7 mmol) in dry THF (20 mL) and the reaction mixture stirred overnight at room temperature. Ether (20 mL) and water (25 mL) were added to the reaction mixture, the organic layer separated, washed with water (25 mL), brine (25 mL), dried ($MgSO_4$), filtered, and concentrated. Flash chromatography (10:1→5:1, hexanes/DCM) afforded 678 mg (1.4 mmol, 74%) of **11** as a white solid, mp 117–118°C, R_f 0.54 (2:1 hexanes/DCM on silica gel 60 F_{254}). ^{1}H NMR (500 MHz, $CDCl_3$) δ 3.29 (2H, s), 4.41 (2H, s), 7.07 (2H, d, J = 8 Hz), 7.19–7.25 (5H, m), 7.26–7.3 (6H, m), 7.44 (6H, m); ^{13}C NMR (125 MHz, $CDCl_3$) δ 33.3, 36.6, 67.5, 126.7, 127.9, 129.1, 129.4, 129.5, 136.4, 137.4, 144.5. Anal. Calcd for $C_{27}H_{23}BrS$: C 70.58, H 5.05, S 6.98. Found: C 70.64, H 5.56, S 6.11.

1-Bromo-9-tritylthiononane (13)—To a solution of 1,9-dibromononane (**12**, 5.72 g, 20 mmol, 4 mL) and trityl mercaptan (2.76 g, 10 mmol) in CH_3CN (50 mL) was added anhydrous K_2CO_3 (10.35 g, 75 mmol) and the mixture stirred overnight at room temperature. The reaction mixture was filtered and the filtrate evaporated under reduced pressure. The residue was subjected to flash chromatography on silica gel eluted with hexanes to give **13** (2.82 g, 5.86 mmol, 59%) as a white solid, mp 58–60°C, R_f 0.48 (3:1 hexanes/DCM on silica gel 60 F_{254}). ^{1}H NMR (500 MHz, $CDCl_3$) δ 1.12–1.28 (8H, m), 1.38 (4H, quintet, J = 7.5 Hz, 7 Hz), 1.82 (2H, quintet, J = 7.5 Hz), 2.12 (2H, t, J = 7.5 Hz), 3.38 (2H, t, J = 7 Hz), 7.17–7.21 (3H, m), 7.24–7.28 (6H, m), 7.39–7.42 (6H, m); ^{13}C NMR (125 MHz, $CDCl_3$) δ 28.1, 28.5, 28.6, 29.0, 29.2, 32.0, 32.8, 33.9, 66.3, 126.4, 127.7, 129.5, 145.0. Anal. Calcd for $C_{28}H_{33}BrS$: C 69.84, H 6.91, S 6.66. Found: C 70.01, H 6.77, S 6.44.

1-Bromo-3-tritylthiopropane (15)—To a solution of 1,3-dibromopropane **14** (8.0 g, 40 mmol, 4 mL) and trityl mercaptan (5.4 g, 20 mmol) in CH_3CN (150 mL) was added anhydrous K_2CO_3 (20.7 g, 150 mmol) and the mixture stirred overnight at room temperature. The reaction mixture was filtered and the filtrate evaporated under reduced pressure. The residue was subjected to flash chromatography on silica gel eluted with hexanes to give **15** (5.1 g, 12.9 mmol, 65%) as a white solid, mp 90–92°C, R_f 0.45 (3:1 hexanes/DCM on silica gel 60 F_{254}). ^{1}H NMR (500 MHz, $CDCl_3$) δ 1.80 (2H, quintet, J = 7 Hz, 6.5 Hz), 2.31 (2H, t, J = 7 Hz), 3.31 (2H, t, J = 6.5 Hz), 7.18–7.23 (3H, m), 7.25–7.29 (6H, m), 7.40–7.41 (6H, m); ^{13}C NMR (125 MHz, $CDCl_3$) δ 30.2, 31.6, 32.2, 66.7, 126.6,

127.8, 129.5, 144.6. Anal. Calcd for $C_{22}H_{21}BrS$: C 66.50, H 5.33, S 8.07. Found: C 66.76, H 5.26, S 7.42.

9-Tritylthio-3,6-dioxanonan-1-ol (16)—To a mixture of NaH (0.25 g, 10.6 mmol) and TBAI (0.19 g, 0.5 mmol) in dry THF (5 mL) was added a solution of diethylene glycol (1.6 g, 15.1 mmol, 1.43 mL) in THF (25 mL) dropwise. After 30 min, a solution of **15** (2.0 g, 5 mmol) in dry THF (30 mL) was added dropwise and the mixture heated at reflux overnight. The reaction mixture was cooled, cautiously quenched with water (50 mL), and the mixture extracted with ether (3 × 50 mL). The combined organic layers were washed with brine, dried ($MgSO_4$), filtered, and concentrated *in vacuo*. The residue was subjected to flash chromatography on silica gel eluted with hexanes/EtOAc (2:1→1:1) to give **16** (0.76 g, 1.8 mmol, 36%) as a white solid, mp 63–64°C, R_f 0.29 (1:1 hexanes/EtOAc on silica gel 60 F_{254}). ^{1}H NMR (500 MHz, $CDCl_3$) δ 1.64 (2H, quintet, J = 7 Hz, 6.5 Hz), 2.23 (2H, t, J = 7 Hz), 2.33 (1H, br s), 3.40 (2H, t, J = 6.5 Hz), 3.50 (2H, m), 3.55–3.60 (4H, m), 3.68 (2H, m), 7.19 (3H, m), 7.26 (6H, m), 7.38–7.42 (6H, m); ^{13}C NMR (125 MHz, $CDCl_3$) δ 28.6, 61.8, 66.5, 69.9, 70.1, 70.3, 72.4, 126.5, 127.7, 129.5, 144.8; HRMS-ESI calculated for $C_{26}H_{30}O_3SNa$ $(M+Na)^+$ 445.1808, found 445.1809. Anal. Calcd for $C_{26}H_{30}O_3S$: C 73.90, H 7.16. Found C 73.52, H 7.19.

1-Bromo-9-tritylthio-3,6-dioxanonane (17)—To a solution of **16** (1.0 g, 2.36 mmol) in DCM (20 mL) was added CBr_4 (0.86 g, 2.60 mmol) followed by PPh_3 (0.68 g, 2.60 mmol) and the mixture stirred at room temperature. After 4 h, the pale brown solution was concentrated under reduced pressure and the residue subjected to flash chromatography on silica gel. Elution with hexanes/EtOAc (85:15) gave **17** (0.88 g, 1.88 mmol, 80%) as a white solid, mp 68–70°C, R_f 0.53 (4:1 hexanes/EtOAc on silica gel 60 F_{254}). ^{1}H NMR (500 MHz, $CDCl_3$) δ 1.64 (2H, quintet, J = 7 Hz, 6.5 Hz), 2.23 (2H, t, J = 7 Hz), 3.38–3.43 (4H, m), 3.49 (2H, m), 3.59 (2H, m), 3.75 (2H, t, J = 6.5 Hz), 7.19 (3H, m), 7.26 (6H, m), 7.40 (6H, m); ^{13}C NMR (125 MHz, $CDCl_3$) δ 28.7, 30.2, 66.4, 69.9, 70.0, 70.4, 71.2, 126.5, 127.7, 129.5, 144.8; HRMS-ESI calculated for $C_{26}H_{29}O_2BrSNa$ $(M+Na)^+$ 507.0964, found 507.0946. Anal. Calcd for $C_{26}H_{29}O_2BrS$: C 64.32, H 6.02. Found: C 64.28, H 6.07.

1,4,7-Tris(*tert*-butoxycarbonylmethyl)-1,4,7,10-tetraazacyclododecane (8).39—To a suspension of cyclen 1**8** (2.00 g, 11.62 mmol) and sodium acetate (2.85 g, 34.8 mmol) in *N*,*N*-dimethyl acetamide (DMA, 25 mL) at 0°C was added a solution of *t*-butyl bromoacetate (6.79 g, 34.82 mmol, 5.14 mL) in DMA (10 mL) dropwise. The reaction mixture was stirred at room temperature for 5 d, after which it was poured into water (125 mL) to give a clear yellow solution. Solid $NaHCO_3$ was added portionwise until **8** precipitated as a white solid. The precipitate was collected by filtration and dissolved in $CHCl_3$ (150 mL). The solution was washed with water (75 mL), dried ($MgSO_4$), filtered, and concentrated to about 20 mL. Ether (150 mL) was added, after which **8** crystallized as a white fluffy solid, mp 201–202°C, R_f 0.37 (10:1 DCM/MeOH on silica gel 60 F_{254}). Yield: 4.7 g (9.1 mmol, 78%). ^{1}H NMR (500 MHz, $CDCl_3$) δ 1.38 (27H, s), 2.78–2.88 (12H, m), 3.01 (4H, m), 3.21 (2H, br s), 3.30 (4H, br s), 10.18 (1H, br s); ^{13}C NMR (125 MHz, $CDCl_3$) δ 28.0, 28.1, 47.4, 48.5, 49.1, 51.0, 51.2, 58.1, 81.4, 81.6, 169.4, 170.3; HRMS-ESI calcd for $C_{26}H_{51}N_4O_6$ $(M+H)^+$ 515.3809, found 515.3817.

1,4,7-Tris(*tert*-butoxycarbonylmethyl)-10-[4-(triphenylmethylthio)methyl)phenyl]methyl-1,4,7,10-tetraazacyclododecane (19a)—To a solution of **8** (2.0 g, 3.9 mmol) in dry CH_3CN (40 mL) were added **11** (1.9 g, 4.1 mmol) and K_2CO_3 (4.3 g, 31.1 mmol) and the mixture heated at 60°C. After 2 h, the reaction mixture was filtered and the filtrate evaporated to dryness under reduced pressure. The residue was dissolved in DCM (100 mL) and the resulting solution was washed with 1N

HCl (2 × 50 mL), saturated aqueous $NaHCO_3$ (50 mL), and brine. The organic layer was dried ($MgSO_4$), filtered, and concentrated *in vacuo*. The residue was subjected to flash chromatography on silica gel eluted with DCM/MeOH (25:1) to give **19a** (2.8 g, 3.14 mmol, 80%) as a white foam, R_f 0.38 (10:1 DCM/MeOH on silica gel 60 F_{254}). ^{1}H NMR (500 MHz, $CDCl_3$) δ 1.43 (9H, br s), 1.46 (18H, br s), 2.20 (4H, m), 2.35 (6H, m), 2.50–2.90 (6H, m), 3.02 (4H, m), 3.23 (2H, m), 7.10 (2H, d, J = 7.5 Hz), 7.22 (2H, m), 7.29 (9H, m), 7.45 (6H, m); ^{13}C NMR (125 MHz, $CDCl_3$) δ 27.8, 27.9, 28.0, 28.1, 36.5, 53.3, 55.6, 55.8, 59.2, 67.2, 82.2, 82.6, 126.6, 127.8, 129.3, 129.4, 130.0, 136.0, 136.3, 144.4, 172.4, 173.3; HRMS-ESI calcd for $C_{53}H_{73}N_4O_6S$ $(M+H)^+$ 893.5251, found 893.5216.

1,4,7-Tris(*tert*-butoxycarbonylmethyl)-10-[9-(triphenylmethylthio)nonyl]-1,4,7,10-tetraaza-cyclododecane (19b)—To a solution of **8** (2.0 g, 3.9 mmol) in dry CH_3CN (40 mL) was added **13** (2.0 g, 4.1 mmol) and K_2CO_3 (4.3 g, 31.1 mmol) and the mixture heated at 60°C. After 4 h, the reaction mixture was filtered and the filtrate evaporated to dryness under reduced pressure. The residue was dissolved in DCM (100 mL) and the resulting solution was washed with 1N HCl (2 × 50 mL), saturated aqueous $NaHCO_3$ (50 mL), and brine. The organic layer was dried ($MgSO_4$), filtered, and concentrated *in vacuo*. The residue was subjected to flash chromatography on silica gel eluted with DCM/MeOH (25:1) to give **19b** (2.84 g, 3.1 mmol, 80%) as a white foam, R_f 0.40 (10:1 DCM/MeOH on silica gel 60 F_{254}). ^{1}H NMR (500 MHz, $CDCl_3$) δ 1.11–1.26 (10H, m), 1.34–1.41 (4H, m), 1.42–1.47 (27H, m), 2.12 (2H, t, J = 7 HZ), 2.25–2.50 (10H, m), 2.79 (4H, m), 3.00–3.22 (6H, m), 3.28 (2H, br s), 3.47 (2H, m), 7.19 (3H, m), 7.23–7.29 (6H, m), 7.36–7.41 (6H, m); ^{13}C NMR (125 MHz,$CDCl_3$) δ 27.7, 27.9, 28.0, 28.1, 28.5, 28.9, 29.0, 29.1, 29.2, 29.3, 29.5, 31.9, 47.7, 50.2, 50.3, 50.5, 52.6, 52.9, 54.4, 55.7, 56.3, 56.8, 66.2, 81.5, 81.6, 82.2, 82.5, 126.3, 127.6, 129.4, 144.8, 169.7, 170.2, 172.4; HRMS-ESI calcd for $C_{54}H_{83}N_4O_6S$ $(M+H)^+$ 915.6028, found 915.6019.

1,4,7-Tris(*tert*-butoxycarbonylmethyl)-10-[9-(triphenylmethylthio)-3,6-dioxanonyl]1,4,7,10-tetraazacyclododecane (19c)—To a solution of **8** (1.72 g, 3.37 mmol) in dry CH_3CN (40 mL) was added **17** (1.73 g, 3.54 mmol) and K_2CO_3 (3.9 g, 28.32 mmol) and the mixture heated at 60°C. After 4 h, the reaction mixture was filtered and the filtrate evaporated to dryness under reduced pressure. The residue was dissolved in 1N HCl (50 mL) and brine (50 mL) and the resulting solution was extracted with DCM (3 × 50 mL). The organic extracts were combined, washed with saturated aqueous $NaHCO_3$ (50 mL), brine, dried ($MgSO_4$), filtered, and concentrated *in vacuo*. The residue was subjected to flash chromatography on silica gel eluted with DCM/MeOH (25:1) to give **19c** (2.84 g, 3.09 mmol, 92%) as a white foam, R_f 0.43 (10:1 DCM/MeOH on silica gel 60 F_{254}). ^{1}H NMR (500 MHz, $CDCl_3$) δ 1.44 (27, m), 1.61 (2H, quintet, J = 7 Hz, 6.5 Hz), 2.20 (2H, t, J = 7 Hz), 2.22–2.50 (8H, cluster of m), 2.82 (8H, m), 3.02 (8H, m), 3.33 (2H, t, J = 6.5 Hz), 3.48 (4H, m), 3.60 (2H, m), 7.20 (3H, m), 7.26 (6H, m), 7.37 (6H, m); ^{13}C NMR (125 MHz, $CDCl_3$) δ 27.9, 28.0, 28.1, 28.2, 28.6, 28.7, 49.7, 50.5, 52.2, 53.4, 55.6, 56.3, 66.5, 67.5, 69.5, 69.9, 70.0, 82.0, 82.1, 126.5, 127.7, 129.4, 144.7, 172.4; HRMS-ESI calcd for $C_{52}H_{79}N_4O_8S$ $(M+H)^+$ 919.5613, found 919.5612.

1,4,7-Tris(carboxymethyl)-10-[4-(thiomethyl)phenyl]methyl-1,4,7,10-tetraazacyclodode-cane (20a)—To a mixture of **19a** (2.0 g, 2.2 mmol), Et_3SiH (0.28 g, 2.4 mmol, 386 μL), and butanethiol (20 mL) was added TFA (20 mL) dropwise. The mixture was stirred overnight at room temperature. Volatiles were removed in vacuo, a minimum amount of MeOH was added to effect a solution, and ether (30 mL) was added. The precipitated white solid was collected by filtration and purified by flash chromatography on silica gel eluted with $CHCl_3$/MeOH/aq. NH_4OH (5:3:1) to give **20a** as a waxy solid (0.85 g, 1.76 mmol, 80%), R_f 0.41 (5:3:1 DCM/MeOH/aq. NH_4OH on silica gel

60 F_{254}). ^{1}H NMR (600 MHz, TFA-*d*) δ 3.21 (4H, m), 3.33 (3H, m), 3.42 (3H, m), 3.58 (4H, m), 3.78 (2H, m), 3.72 (2H, m), 3.77 (4H, m), 3.87 (2H, br s), 4.44 (2H, br s), 4.66 (2H, br s); ^{13}C NMR (150 MHz, TFA-*d*) δ 29.1, 49.9, 50.3, 51.7, 54.1, 54.5, 56.4, 60.7, 127.4, 131.5, 133.1, 146.9, 171.0, 177.4; HRMS-ESI calcd for $C_{20}H_{35}N_4O_6S$ $(M+H)^+$ 483.2277, found 483.2273.

[1,4,7-Tris(carboxymethyl)-10-(9-mercaptononyl)-1,4,7,10-tetraazacyclododecane (20b)—To a mixture of **19b** (2.16 g, 2.36 mmol), Et_3SiH (0.30 g, 2.6 mmol, 415 μL), and butanethiol (20 mL) was added TFA (20 mL) dropwise. The mixture was stirred overnight at room temperature. Volatiles were removed in vacuo, a minimum amount of MeOH was added to effect a solution, and ether (30 mL) was added. The precipitated white solid was collected by filtration and purified by flash chromatography on silica gel eluted with $CHCl_3$/MeOH/aq. NH_4OH (5:3:1) to give **20b** as a waxy solid (0.88 g, 1.74 mmol, 74%), R_f 0.54 (5:3:1 DCM/MeOH/aq. NH_4OH on silica gel 60 F_{254}). ^{1}H NMR (500 MHz, TFA-*d*) δ 1.43 (12H, m), 1.72 (2H, m), 1.86 (2H, m), 2.67 (1H, m), 3.13–3.22 (4H, m), 3.30–3.45 (6H, m), 3.57 (4H, br s), 3.67–3.84 (8H, m), 4.34 (2H, br s); ^{13}C NMR (125 MHz, $CDCl_3$) δ 25.3, 25.8, 28.1, 29.8, 30.4, 30.6, 30.8, 35.0, 50.3, 50.9, 52.0, 54.5, 54.7, 56.5, 57.6, 171.4, 178.2; HRMS-ESI calcd for $C_{23}H_{45}N_4O_6S$ $(M+H)^+$ 505.3059, found 505.3052.

1,4,7-Tris(carboxymethyl)-10-(9-mercapto-3,6-dioxanonyl)-1,4,7,10-tetraazacyclododecane (20c)—To a mixture of **19c** (2.4 g, 2.6 mmol), Et_3SiH (0.34 g, 2.9 mmol, 460 μL), and butanethiol (25 mL) was added TFA (25 mL) dropwise. The mixture was stirred overnight at room temperature. Volatiles were removed in vacuo, a minimum amount of MeOH was added to effect a solution, and ether (30 mL) was added. The precipitated white solid was collected by filtration and purified by flash chromatography on silica gel eluted with $CHCl_3$/MeOH/aq. NH_4OH (5:3:1) to afford **20c** as a waxy solid (0.98 g, 1.92 mmol, 74%), R_f 0.52 (5:3:1 DCM/MeOH/aq. NH_4OH on silica gel 60 F_{254}). ^{1}H NMR (500 MHz, TFA-*d*) δ 1.89 (2H, m), 2.2 (1H, t, J = 7 Hz), 2.95–3.18 (8H, m), 3.45 (2H, m), 3.54–3.75 (18H, m), 3.85 (3H, m), 4.21 (2H, br s); ^{13}C NMR (125 MHz, $CDCl_3$) δ 21.8, 33.6, 50.1, 50.7, 53.1, 54.4, 54.7, 56.4, 56.6, 66.0, 70.9, 71.6, 71.9, 170.9, 177.4; HRMS-ESI calcd for $C_{21}H_{41}N_4O_6S$ $(M+H)^+$ 508.2640, found 508.2634.

{1,4,7-Tris(carboxymethyl)-10-[4-(thiomethyl)phenyl]methyl-1,4,7,10-tetraazacyclododec-anato}gadolinium (3a)—To a solution of **20a** (100 mg, 0.207 mmol) in MeOH (3 mL) was added $Gd(OAc)_3$ (69.2 mg, 0.207 mmol) and the mixture heated at reflux. After 2 h volatiles were removed in vacuo. The residue was subjected to flash chromatography on reverse-phase silica gel 60 RP-18 eluted with MeOH/H_2O (7:3) to give **3a** as a white solid (0.1 g, 0.15 mmol, 75%), R_f 0.16 (MeOH/H_2O 19:1 on silica gel 60 RP-18 F_{254}); ESI-MS calcd for $C_{20}H_{32}GdN_4O_6S$ $(M+H)^+$ 638.1287, found 638.1307.

[1,4,7-Tris(carboxymethyl)-10-(9-mercaptononyl)-1,4,7,10-tetraazacyclododecanato] gadolinium (4a)—To a solution of **20b** (100 mg, 0.198 mmol) in MeOH (3 mL) was added $Gd(OAc)_3$ (66.2 mg, 0.198 mmol) and the mixture heated at reflux. After 2 h volatiles were removed in vacuo. The residue was subjected to flash chromatography on reverse-phase silica gel 60 RP-18 eluted with MeOH/H_2O (7:3) to give **4a** as a white solid (75 mg, 0.113 mmol, 57%), R_f 0.17 (MeOH/H_2O 19:1 on silica gel 60 RP-18 F_{254}); ESI-MS calcd for $C_{23}H_{42}GdN_4O_6S$ $(M+H)^+$ 660.2061, found 660.2069. Crystals were grown for X-ray diffraction analysis according to a procedure used previously for growing an In-DO3A-TPP complex.41 An equimolar mixture of **20b** and $Gd(OAc)_3$ was heated at 100°C for 30 min in NH_4OAc buffer (0.5 M, pH = 6). Slow diffusion of acetone into the reaction mixture produced colorless, flat plates.

{1,4,7-Tris(carboxymethyl)-10-[(9-mercapto-3,6-dioxa)nonyl]-1,4,7,10-tetraazacyclo-dodecanato}gadolinium (5a)—To a solution of **20c (**100 mg, 0.196 mmol) in MeOH (3 mL) was added $Gd(OAc)_3$ (65.8 mg, 0.196 mmol) and the mixture heated at reflux. After 2 h volatiles were removed in vacuo. The residue was subjected to flash chromatography on reverse-phase silica gel 60 RP-18 eluted with $MeOH/H_2O$ (1:4) to give **5a** as a white solid (0.1 g, 0.15 mmol, 75%), R_f 0.23 ($MeOH/H_2O$ 1:4 on silica gel 60 RP-18 F_{254}); ESI-MS calcd for $C_{21}H_{38}GdN_4O_8S$ $(M+H)^+$ 664.1646, found 664.1650.

{1,4,7-Tris(carboxymethyl)-10-[4-(thiomethyl)phenyl]methyl-1,4,7,10-tetraazacyclododec-anato}europium (3b)—To a solution of **20a** (100 mg, 0.207 mmol) in MeOH (3 mL) was added $Eu(OAc)_3$ (68.3 mg, 0.207 mmol) and the mixture heated at reflux. After 2 h volatiles were removed in vacuo. The residue was subjected to flash chromatography on reverse-phase silica gel 60 RP-18 eluted with $MeOH/H_2O$ (7:3) to give **3b** as a white solid (93 mg, 0.147 mmol, 71%), R_f 0.13 ($MeOH/H_2O$ 19:1 on silica gel 60 RP-18 F_{254}); ESI-MS calcd for $C_{20}H_{32}EuN_4O_6S$ $(M+H)^+$ 633.1259, found 633.1243.

[1,4,7-Tris(carboxymethyl)-10-(9-mercaptononyl)-1,4,7,10-tetraazacyclododecanato]-europium (4b)—To a solution of **20b** (100 mg, 0.198 mmol) in MeOH (3 mL) was added $Eu(OAc)_3$ (65.3 mg, 0.198 mmol) and the mixture heated at reflux. After 2 h volatiles were removed in vacuo. The residue was subjected to flash chromatography on reverse-phase silica gel 60 RP-18 eluted with $MeOH/H_2O$ (7:3) to give **4b** as a white solid (75 mg, 0.114 mmol, 58%), R_f 0.10 ($MeOH/H_2O$ 19:1 on silica gel 60 RP-18 F_{254}); ESI-MS calcd for $C_{23}H_{42}EuN_4O_6S$ $(M+H)^+$ 655.2032, found 655.2035.

{1,4,7-Tris(carboxymethyl)-10-[(9-mercapto-3,6-dioxa)nonyl]-1,4,7,10-tetraazacyclo-dodecanato}europium (5b)—To a solution of **20c** (100 mg, 0.196 mmol) in MeOH (3 mL) was added $Eu(OAc)_3$ (64.8 mg, 0.196 mmol) and the mixture heated at reflux. After 2 h volatiles were removed in vacuo. The residue was subjected to flash chromatography on reverse-phase silica gel 60 RP-18 eluted with $MeOH/H_2O$ (1:4) to give **5b** as a white solid (106 mg, 0.161 mmol, 82%), R_f 0.20 ($MeOH/H_2O$ 1:4 on silica gel 60 RP-18 F_{254}); ESI-MS calcd for $C_{21}H_{38}EuN_4O_6S$ $(M+H)^+$ 659.1617, found 659.1617.

1-Bromo-3,6-dioxanonane (21)—To a solution of diethylene glycol monopropyl ether (5.0 g, 30 mmol) in DCM (150 mL) was added CBr_4 (12.3 g, 37 mmol) followed by PPh_3 (9.7 g, 37 mmol). The mixture stirred at room temperature. After 12 h, the pale brown solution was concentrated in vacuo and the residue subjected to flash chromatography on silica gel. Elution with hexanes/EtOAc (80:20) gave **21** (5.7 g, 27 mmol, 90%) as a colorless oil, R_f 0.54 (4:1 hexanes/EtOAc on silica gel 60 F_{254}). ^1H NMR (500 MHz, $CDCl_3$) δ 0.92 (2H, t, J = 6.5 Hz), 1.61 (2H, m), 3.43 (2H, m), 3.47 (2H, m), 3.59 (2H, m), 3.67 (2H, m), 3.82 (2H, t, J = 6.5 Hz); ^{13}C NMR (125 MHz, $CDCl_3$) δ 10.4, 22.8, 30.2, 70.0, 70.5, 71.2.

1,4,7-Tris(*tert*-butoxycarbonylmethyl)-10-(3,6-dioxanonyl)-1,4,7,10-tetraazacyclododecane (22)—To a solution of **8** (2.0 g, 4 mmol) in dry CH_3CN (40 mL) were added **21** (0.88 g, 4.2 mmol) and K_2CO_3 (4.4 g, 32 mmol) and the mixture heated at 60°C. After 12 h, the reaction mixture was filtered and the filtrate evaporated to dryness in vacuo. The residue was dissolved in 1N HCl (50 mL) and brine (50 mL) and the resulting solution was extracted with DCM (3 × 50 mL). The organic extracts were combined, washed with saturated aqueous $NaHCO_3$ (50 mL), brine, dried ($MgSO_4$), filtered, and concentrated *in vacuo*. The residue was subjected to flash chromatography on silica gel eluted with DCM/MeOH (25:1) to give **22** (2.47 g, 3.8 mmol, 96%) as a white foam, R_f 0.52 (10:1 DCM/MeOH on silica gel 60 F_{254}). ^1H NMR (500 MHz, $CDCl_3$) δ 0.89 (3H, t, J = 7.5 Hz), 1.45 (27, m), 1.55 (2H, m), 2.22–2.60 (8H, cluster of m), 2.70–2.90 (10H, m), 3.05 (4H, m), 3.33

(2H, m), 3.50 (4H, m), 3.70 (4H, m); ^{13}C NMR (125 MHz, $CDCl_3$) δ 10.5, 22.7, 27.9, 28.0, 28.1, 28.2, 49.8, 50.4, 52.2, 55.7, 56.4, 67.5, 69.3, 69.9, 70.1, 82.0, 82.1, 172.4, 172.7; HRMS-ESI calcd for $(M+H)^+$ $C_{33}H_{65}N_4O_8$ 645.4796, found 645.4799.

1,4,7-Tris(carboxymethyl)-10-(3,6-dioxanonyl)-1,4,7,10-tetraazacyclododecane (23)—To a solution of **22** (0.60 g, 0.93 mmol) in DCM (4 mL) was added TFA (4 mL) dropwise. The mixture was stirred overnight at room temperature. Volatiles were removed in vacuo and the residue was subjected to flash chromatography on silica gel eluted with $CHCl_3$/MeOH/aq. NH_4OH (4:2:1) to afford **23** as a waxy solid (0.34 g, 0.72 mmol, 77%), R_f 0.54 (4:2:1 DCM/MeOH/aq. NH_4OH on silica gel 60 F_{254}). ^{1}H NMR (500 MHz, *TFA-d)* δ 1.03 (3H, t, J = 7 Hz), 1.79 (2H, m), 3.15–3.29 (4H, m), 3.30–3.42 (4H, m), 3.68 (2H, m), 3.7–3.8 (8H, m), 3.88 (2H, m), 3.93 (2H, m), 4.08 (2H, m), 4.45 (2H, br s); ^{13}C NMR (125 MHz, $CDCl_3$) δ 10.8, 23.9, 50.7, 51.3, 53.9, 55.0, 55.2, 57.1, 57.3, 67.0, 71.2, 72.5, 76.2, 171.9, 178.3; HRMS calcd for $(M+H)^+$ $C_{21}H_{41}N_4O_8$ 477.2918, found 477.2926.

[1,4,7-Tris(carboxymethyl)-10-(3,6-dioxa)nonyl-1,4,7,10-tetraazacyclododecanato] gadolinium (24)—To a solution of **23 (**100 mg, 0.21 mmol) in MeOH (3 mL) was added $Gd(OAc)_3$ (70.2 mg, 0.21 mmol) and the mixture heated at reflux. After 2 h volatiles were removed in vacuo. The residue was subjected to flash chromatography on reverse-phase silica gel 60 RP-18 eluted with MeOH/H_2O (1:4) to give **24** as a white solid (120 mg, 0.19 mmol, 75%), R_f 0.25 (MeOH/H_2O 3:7 on silica gel 60 RP-18 F_{254}); ESI-MS calcd for $C_{21}H_{39}GdN_4O_6$ $(M+H)^+$ 632.1930, found 632.1932.

Binding of Gd-thiols to Human Serum Albumin

Solutions of Gd complexes were made in either phosphate-buffered saline (PBS), acetate-buffered saline, or HEPES-buffered saline, and in corresponding solutions that contained 0.66 mM human serum albumin (HSA, Sigma), as well as 0–2.0 mM homocysteine (Sigma), to final gadolinium concentrations of 0–1.0 mM. All solutions also contained 10 mM sodium azide, and the final pH of all solutions was 7.40 ± 0.05 at room temperature. Solutions were allowed to equilibrate overnight at 37°C prior to measurements. Aliquots (500 μ*L)* of each solution containing HSA were placed in pre-warmed ultrafiltration units (Amicon UItra-4 Centrifugal Filter Units, 30000 MW cutoff, Millipore Corporation) and immediately centrifuged at 7451 g for 10.7 min, inclusive of braking time. It was assumed that gadolinium bound to HSA (Gd_{bound}) would not pass through the membrane, and that gadolinium in the filtrate (Gd_{free}) accurately represented the unbound gadolinium in each sample. Gadolinium concentrations in the filtrates were determined by MRI relaxometry. The apparent equilibrium binding constant (K_A) for each complex was calculated from the Law of Mass Action.52

Relaxivity of Gd complexes in the absence of HSA

Measurements of the longitudinal water-proton relaxivities of Gd complexes in buffered saline were made at 37°C on a 7 T Bruker Biospec MR Instrument (Bruker Biospin, Billerica, MA). 96-Well tissue culture plates (Falcon) were cut down to 6×8 wells, creating a sample tray which fit inside a 72 mm ID birdcage radio-frequency transmitter-receiver coil (Bruker). Aliquots (250 μL) of the gadolinium solutions were loaded into these wells. Spaces between the wells were filled with water in order to reduce air-water susceptibility artifacts in the images. The sample tray was maintained at 37°C during imaging by flowing heated air over the sample tray. Sample temperature was continuously monitored using a fluoroptic temperature probe (Luxtron Corporation, Santa Clara, CA, USA). Spin-echo MR images of cross-sections of the wells were acquired with recycle times (T_R) ranging between 35–8000 ms, and an echo time (T_E) of 4 ms. Signal intensity *S* in each well was fitted to Eq.

[1] to extract the T_1 at each solution condition. The factor *c* was between 0.98–1.0 in all regressions.

$$S = S_0\left(1 - c \cdot \exp\left[\frac{-T_R}{T_1}\right]\right) \quad [1]$$

The T_1 relaxation times of the solutions of gadolinium in saline containing 0–2.0 mM homocysteine thus calculated were then fit to Eq. [2], and a longitudinal relaxivity r_1 obtained for each solution condition.

$$\frac{1}{T_1} = \frac{1}{T_{10}} + r_1 \cdot [\mathrm{Gd}] \quad [2]$$

Here $1/T_{10}$ is the relaxation rate in the absence of contrast agent, and [Gd] is the concentration of gadolinium in the solution.

Relaxivity of Gd complexes in the presence of HSA

The relaxivity of gadolinium in HSA-containing solutions was approximated to have only two components: “free” (monomer, homodimer, heterodimer), and “bound” (to HSA). The T_1 times of the solutions of both gadolinium complexes in saline + HSA were inserted into Eq. [3] and fitted for the relaxivity of bound gadolinium, r_1(bound)

$$\frac{1}{T_1} = \frac{1}{T_{10}} + r_1(\mathrm{free}) \cdot [\mathrm{Gd(free)}] + r_1(\mathrm{bound}) \cdot [\mathrm{Gd(total)} - \mathrm{Gd(free)}] \quad [3]$$

where [Gd(free)] was obtained as described previously31 with K_A constrained to equal the binding constant calculated for the respective HSA-containing solution. In these regressions, r_1(free) was constrained to equal the relaxivity measured in the corresponding HSA-free solution.

Supplementary Material

Refer to Web version on PubMed Central for supplementary material.

Acknowledgments

This work was supported by grants R01-CA118359 and P30-CA023074 from the National Institutes of Health. The single crystal X-ray diffractometer was purchased with funds from grant CHE-9610347 from the National Science Foundation.

References and Notes

1. Lauffer RB. Paramagnetic Metal Complexes as Water Proton Relaxation Agents for NMR Imaging: Theory and Design. Chem. Rev. 1987; 87:901–927.
2. Tóth É, Helm L, Merbach AE. Relaxivity of MRI Contrast Agents. Top. Curr. Chem. 2002; 221:61–101.
3. Westbrook, C.; Roth, CK.; Talbot, J. MRI in Practice. 3rd ed. Malden, MA: Blackwell; 2005.
4. Caravan P, Ellison JJ, McMurry TJ, Lauffer RB. Gadolinium(III) Chelates as MRI Contrast Agents: Structure, Dynamics, and Applications. Chem. Rev. 1999; 99:2293–2352. [PubMed: 11749483]
5. Caravan P. Strategies for Increasing the Sensitivity of Gadolinium Based MRI Contrast Agents. Chem. Soc. Rev. 2006; 35:512–523. [PubMed: 16729145]

6. Hermann P, Kotek J, Kubìcek V, Lukes I. Gadolinium(III) Complexes as MRI Contrast Agents: Ligand Design and Properties of the Complexes. Dalton Trans. 2008:3027–3047. [PubMed: 18521444]
7. Aime S, Castelli DD, Terreno E. Novel pH-Reporter MRI Contrast Agents. Angew. Chem., Int. Ed. 2002; 41:4334–4336.
8. Lowe MP, Parker D, Reany O, Aime S, Botta M, Castellano G, Gianolio E, Pagliarin R. pH-Dependent Modulation of Relaxivity and Luminescence in Macrocyclic Gadolinium and Europium Complexes Based on Reversible Intramolecular Sulfonamide Ligation. J. Am. Chem. Soc. 2001; 123:7601–7609. [PubMed: 11480981]
9. Zhang S, Wu K, Sherry AD. A Novel pH-Sensitive MRI Contrast Agent. Angew. Chem., Int. Ed. 1999; 38:3192–3194.
10. Aime S, Crich SG, Botta M, Glovenzana G, Palmisano G, Sisti MA. Macromolecular Gd(III) Complex as pH-responsive Relaxometric Probe for MRI Applications. Chem. Commun. 1999:1577–1578.
11. Burai L, Scopelliti R, Tóth ÉE. Eu^{II}-cryptate with Optimal Water Exchange and Electronic Relaxation: A Synthon for Potential pO_2 Responsive Macromolecular MRI Contrast Agents. Chem. Commun. 2002:2366–2367.
12. Aime S, Botta M, Gianolio E, Terreno E. A $p(O_2)$-Responsive MRI Contrast Agent Based on the Redox Switch of Manganese(II/III)-Porphyrin Complexes. Angew. Chem., Int. Ed. 2000; 39:747–750.
13. Que EL, Gianolio E, Baker SL, Wong AP, Aime S, Chang CJ. Copper-Responsive Magnetic Resonance Imaging Contrast Agents. J. Am. Chem. Soc. 2009; 131:8527–8536. [PubMed: 19489557]
14. Mishra A, Fousková P, Angelovski G, Balogh E, Mishra AK, Logothetis NK, Tóth É. Facile Synthesis and Relaxation Properties of Novel Bispolyazamacrocyclic Gd3+ Complexes: An Attempt Towards Calcium-Sensitive MRI Contrast Agents. Inorg. Chem. 2008; 47:1370–1381. [PubMed: 18166011]
15. Hanaoka K, Kikuchi K, Urano Y, Nagano T. Selective Sensing of zinc ions with a Novel Magnetic Resonance Imaging Contrast Agent. J. Chem. Soc., Perkin Trans. 2. 2001:1840–1843.
16. Li W-H, Fraser SE, Meade TJ. A Calcium-Sensitive Magnetic Resonance Imaging Contrast Agent. J. Am. Chem. Soc. 1999; 121:1413–1414.
17. Louie AY, Huber MM, Ahrens ET, Rothbacher U, Moats R, Jacobs RE, Fraser SE, Meade TJ. In vivo Visualization of Gene Expression using Magnetic Resonance Imaging. Nat. Biotechnol. 2000; 18:321–325. [PubMed: 10700150]
18. Duimstra JA, Femia FJ, Meade TJ. A Gadolinium Chelate for Detection of β-Glucuronidase: A Self-Immolative Approach. J. Am. Chem. Soc. 2005; 127:12847–12855. [PubMed: 16159278]
19. Moats RA, Fraser SE, Meade TJ. A Smart Magnetic Resonance Imaging Agent that Reports on Specific Enzymatic Activity. Angew Chem., Int. Ed. 1997; 36:726–728.
20. Tu C, Nagao R, Louie AY. Multimodal Magnetic-Resonance/Optical-Imaging Contrast Agent Sensitive to NADH. Angew Chem., Int. Ed. 2009; 48:6547–6551.
21. Tu C, Louie AY. Photochromically-Controlled, Reversibly-Activated MRI and Optical Contrast Agent. Chem. Commun. 2007:1331–1333.
22. Schulze PC, Yoshioka J, Takahashi T, He Z, King GL, Lee RT. Hyperglycemia Promotes Oxidative Stress through Inhibition of Thioredoxin Function by Thioredoxin-interacting Protein. J. Biol. Chem. 2004; 279:30369–30374. [PubMed: 15128745]
23. Yoh K, Hirayama A, Ishizaki K, Yamada A, Takeuchi M, Yamagichi S, Morito N, Nakano T, Ojima M, Shimohata H, Itoh K, Takahashi S, Yamamoto M. Hyperglycemia Induces Oxidative and Nitrosative Stress and Increases Renal Functional Impairment in Nrf2-Deficient Mice. Genes to Cells. 2008; 13:1159–1170. [PubMed: 19090810]
24. Wu WS. The Signaling Mechanism of ROS in Tumor Progression. Cancer Metastasis Rev. 2006; 25:695–705. [PubMed: 17160708]
25. Lau A, Villeneuve NF, Sun Z, Wong PK, Zhang DD. Dual Roles of Nrf2 in Cancer. Pharmacol. Res. 2008; 58:262–270. [PubMed: 18838122]

26. Hayes JD, McMahon M. NRF2 and KEAP1 Mutations: Permanent Activation of an Adaptive Response in Cancer. TIBS. 2009; 34:176–188. [PubMed: 19321346]
27. Biaglow JE, Varnes ME, Clark EP, Epp ER. The Role of Thiols in Cellular Response to Radiation and Drugs. Radiat. Res. 1983; 95:437–455. [PubMed: 6684310]
28. Fahey RC, Prise KM, Stratford MRL, Watfa RR, Michael BD. Rates for Repair of pBR 322 DNA Radicals by Thiols as Measured by the Gas Explosion Technique: Evidence that Counter-Ion Condensation and Co-Ion Depletion are Significant at Physiological Ionic Strength. Int. J. Radiat. Biol. 1991; 59:901–917. [PubMed: 1674275]
29. Pompella A, De Tata V, Paolicchi A, Zunino F. Expression of γ-Glutamyltransferase in Cancer Cells and its Significance in Drug Resistance. Biochem. Pharmacol. 2006; 71:231–238. [PubMed: 16303117]
30. Anderson CL, Iyer SS, Ziegler TR, Jones DP. Control of Extracellular Cysteine/Cystine Redox State by HT-29 Cells is Independent of Cellular Glutathione. Am. J. Physiol. Regul. Integr. Comp. Physiol. 2007; 293:R1069–R1075. [PubMed: 17567723]
31. Raghunand N, Jagadish B, Trouard TP, Galons J–P, Gillies RJ, Mash EA. Redox-sensitive Contrast Agents for MRI Based on Reversible Binding of Thiols to Serum Albumin. Magn. Reson. Med. 2006; 55:1272–1280. [PubMed: 16700014]
32. Lacerda S, Campello MP, Marques F, Gano L, Kubícek V, Fousková P, Tóth É, Santos I. A Novel Tetraazamacrocycle Bearing a Thiol Pendant Arm for Labeling Biomolecules with Radiolanthanides. Dalton Trans. 2009:4509–4518. [PubMed: 19488449]
33. Marradi M, Alcántara D, de la Fuente JM, García-Martín ML, Cerdán S, Penadés S. Paramagnetic Gd-based Gold Glyconanoparticles as Probes for MRI: Tuning Relaxivities with Sugars. Chem. Commun. 2009:3922–3924.
34. Sugio S, Kashima A, Mochizuki S, Noda M, Kobayashi K. Crystal Structure of Human Serum Albumin at 2.5 Å Resolution. Protein Eng. 1999; 12:439–446. [PubMed: 10388840]
35. Insight II 2005L modeling software was obtained from Accelrys Inc. San Diego CA.
36. Bugaut A, Jantos K, Wietor J-L, Rodriguez R, Sanders JKM, Balasubramanian S. Exploring the Differential Recognition of DNA G-Quadruplex Targets by Small Molecules Using Dynamic Combinatorial Chemistry. Angew. Chem., Int. Ed. 2008; 47:2677–2680.
37. Bowen ME, Monguchi Y, Sankaranarayanan R, Vagner J, Begay LJ, Xu L, Jagadish B, Hruby VJ, Gillies RJ, Mash EA. Design, Synthesis, and Validation of a Branched Flexible Linker for Bioactive Peptides. J. Org. Chem. 2007; 72:1675–1680. [PubMed: 17279799]
38. Appel R. Tertiary Phosphane/Tetrachloromethane, A Versatile Reagent for Chlorination, Dehydration and P-N Linkage. Angew. Chem. Int. Ed. Engl. 1975; 14:801–811.
39. Axelsson O, Olsson A. Synthesis of Cyclen Derivatives. WO 2006112723 A1; CAN. 145:419189.
40. Lin Y, Favre-Reguillon A, Pellet-Rostaing S, Lemaire M. Synthesis of Pyridine-Based Polyaminocarboxylic Ligands Bearing a Thioalkyl Anchor. Tetrahedron Lett. 2007; 48:3463–3466.
41. Yang C-T, Li Y, Liu S. Synthesis and Structural Characterization of Complexes of a DO3A–Conjugated Triphenylphosphonium Cation with Diagnostically Important Metal Ions. Inorg. Chem. 2007; 46:8988–8997. [PubMed: 17784751]
42. Spek AL. Single-crystal structure validation with the program *PLATON*. J. Appl. Cryst. 2003; 36:7–13.
43. Crystal data for **4a**: $C_{25}H_{52}GdN_5O_{10}S$; M = 772.04 g mol^{-1}, T = 223(2) K, Mo Kα, thin colorless plates, triclinic, P-1, a = 8.0364(13) Å, b = 10.4906(17) Å, c = 21.799(4) Å, α = 76.573(3)°, β = 86.307(3)°, γ = 88.816(3)°, V = 1783.8(5) Å^3, Z = 2, 6582 reflections, R_{int} 0.0216, GOF on F^2 = 1.074, R_1 = 0.0275 and wR_2 = 0.0672 ([F^2 >2σ]), R_1 = 0.0331 and wR_2 = 0.0690 (all data).
44. Sengupta S, Chen H, Togawa T, DiBello PM, Majors AK, Büdy B, Ketterer ME, Jacobsen DW. Albumin Thiolate Anion is an Intermediate in the Formation of Albumin-S– S-Homocysteine. J. Biol. Chem. 2001; 276:30111–30117. [PubMed: 11371573]
45. Franklin JL, Lumpkin HE. Some C–S, H–S and S–S Bond Strengths by the Electron Impact Method. J. Am. Chem. Soc. 1952; 74:1023–1026.

46. Yerly F, Borel A, Helm L, Merbach AE. MD Simulations of Acyclic and Macrocylic Gd^{3+}-Based MRI Contrast Agents: Influence of the Internal Mobility on Water Proton Relaxivity. Chem. Eur. J. 2003; 9:5468–5480.

47. Aime S, Gianolio E, Terreno E, Giovenzana GB, Pagliarin R, Sisti M, Palmisano G, Botta M, Lowe MP, Parker D. Ternary Gd(III)L-HSA Adducts: Evidence for the Replacement of Inner-Sphere Water Molecules by Coordinating Groups of the Protein. Implications for the Design of Contrast Agents for MRI. J. Biol. Inorg. Chem. 2000; 5:488–497. [PubMed: 10968620]

48. Botta M, Quici S, Pozzi G, Marzanni G, Pagliarin R, Barra S, Crich SG. NMR Relaxometric Study of New Gd^{III} Macrocyclic Complexes and their Interaction with Human Serum Albumin. Org. Biomol. Chem. 2004; 2:570–577. [PubMed: 14770236]

49. Terreno E, Boniforte P, Botta M, Fedeli F, Milone L, Mortillaro A, Aime S. The Water-Exchange Rate in Neutral Heptadentate DO3A–Like Gd^{III} Complexes: Effect of the Basicity at the Macrocyclic Nitrogen Site. Eur. J. Inorg. Chem. 2003:3530–3533.

50. Discover_3 ESFF (extensible systematic force field). Molecular mechanics force fields, Insight II, 2005L. San Diego: Accelrys, Inc.;

51. The General Experimental Section appears in the Supporting Information that accompanies this article. The purities of synthetic intermediates were estimated to be ≥95% based on elemental analyses and/or thin-layer chromatographic analyses. The purities of compounds **3a–5a, 3b–5b**, and **24** were estimated to be ≥95% based on thin-layer chromatographic analyses.

52. Motulsky, H.; Christopoulos, A. Fitting Models to Biological Data using Linear and Nonlinear Regression. A Practical Guide to Curve Fitting. San Diego: GraphPad Software, Inc.; 2003. p. 187-191.

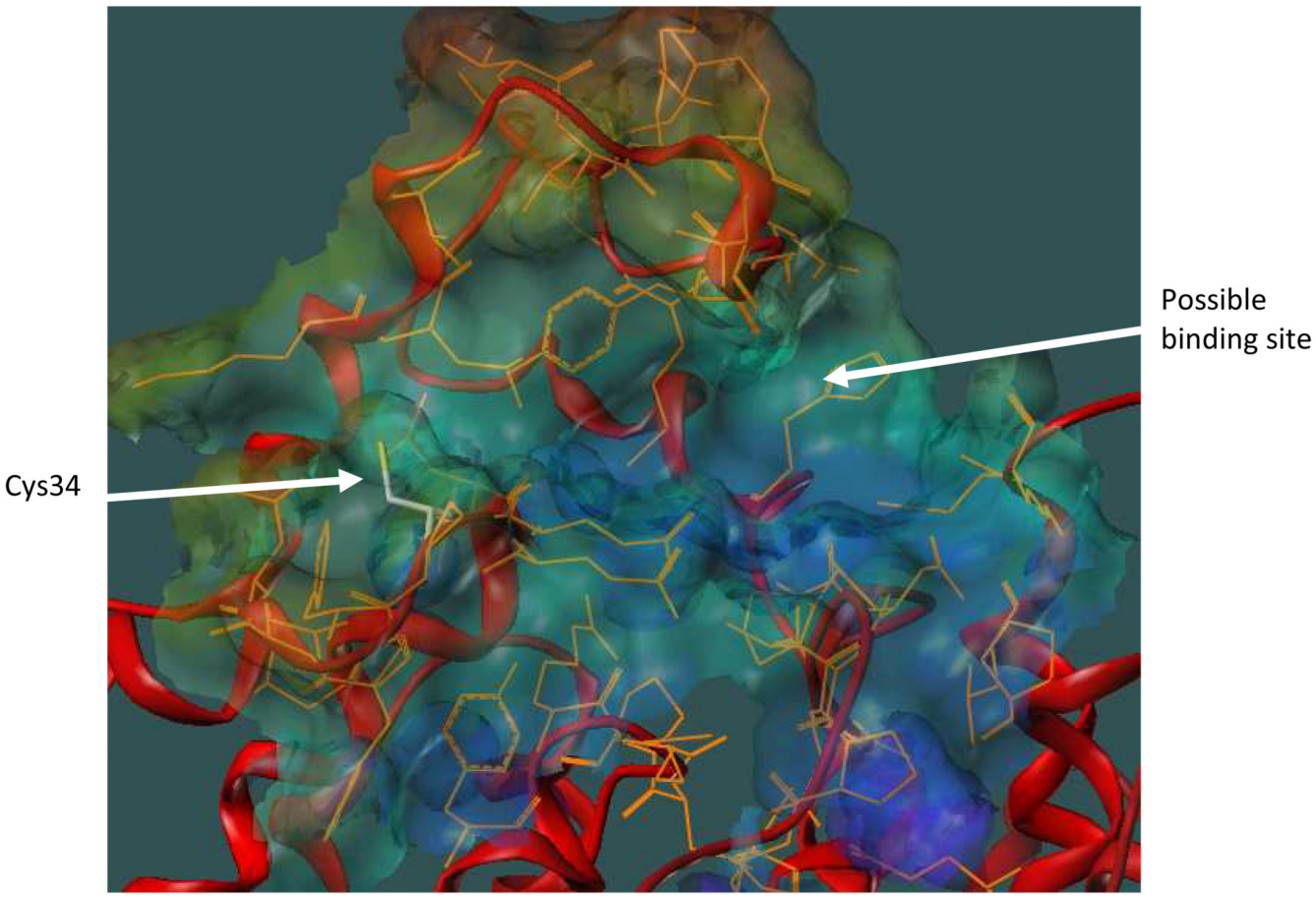

Figure 1.
HSA with the putative binding region shown as a MOLCAD surface. The protein backbone is depicted as a red ribbon and residues that constitute the binding region are shown in orange. Cys34 is displayed as atom-colored sticks.

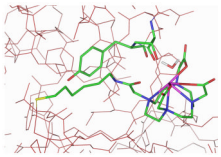

Figure 2.
Docking of **2** with HSA. Compound **2**, HSA residues Thr83 and Tyr84, and a bound water molecule (2.71 Å from Gd) are displayed as atom-colored sticks. Hydrogen atoms and remaining water molecules are omitted for clarity.

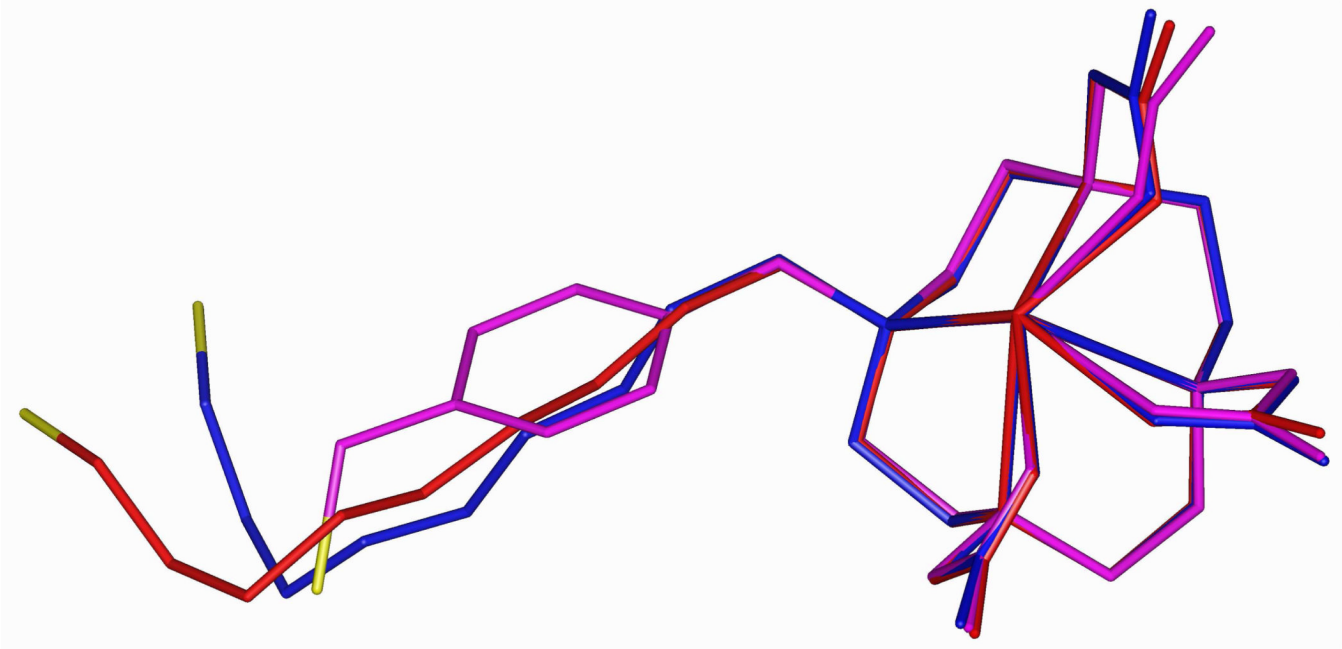

Figure 3.
Overlay of energy-minimized structures for compounds **3a** (magenta), **4a** (red), and **5a** (blue). Sulfur is colored yellow, and hydrogen atoms are omitted for clarity.

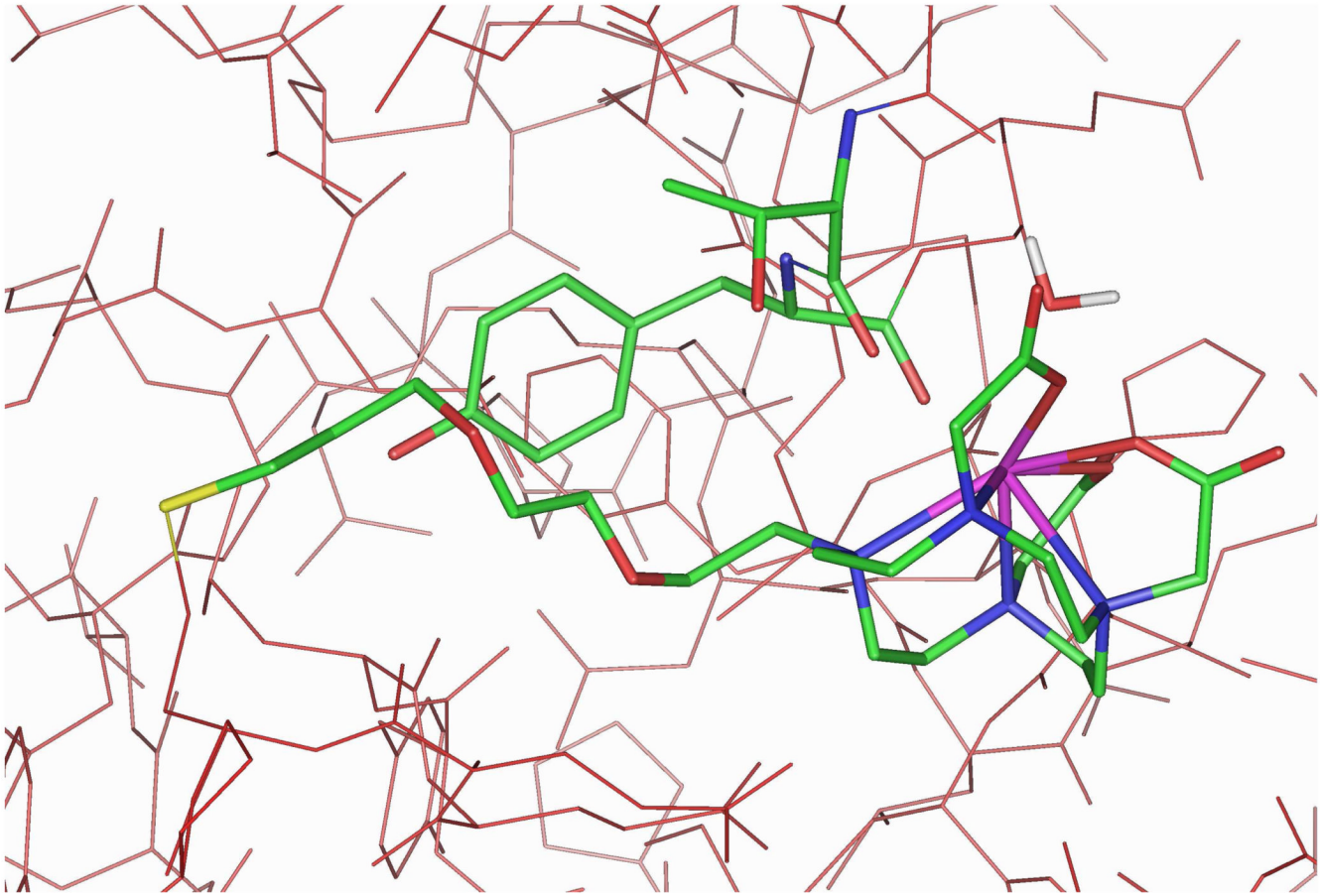

Figure 4.
Docking of **5a** with HSA. Compound **5a**, HSA residues Thr83 and Tyr84, and a bound water molecule (2.67 Å from Gd) are displayed as atom-colored sticks. Hydrogen atoms and the remaining water molecules are omitted for clarity.

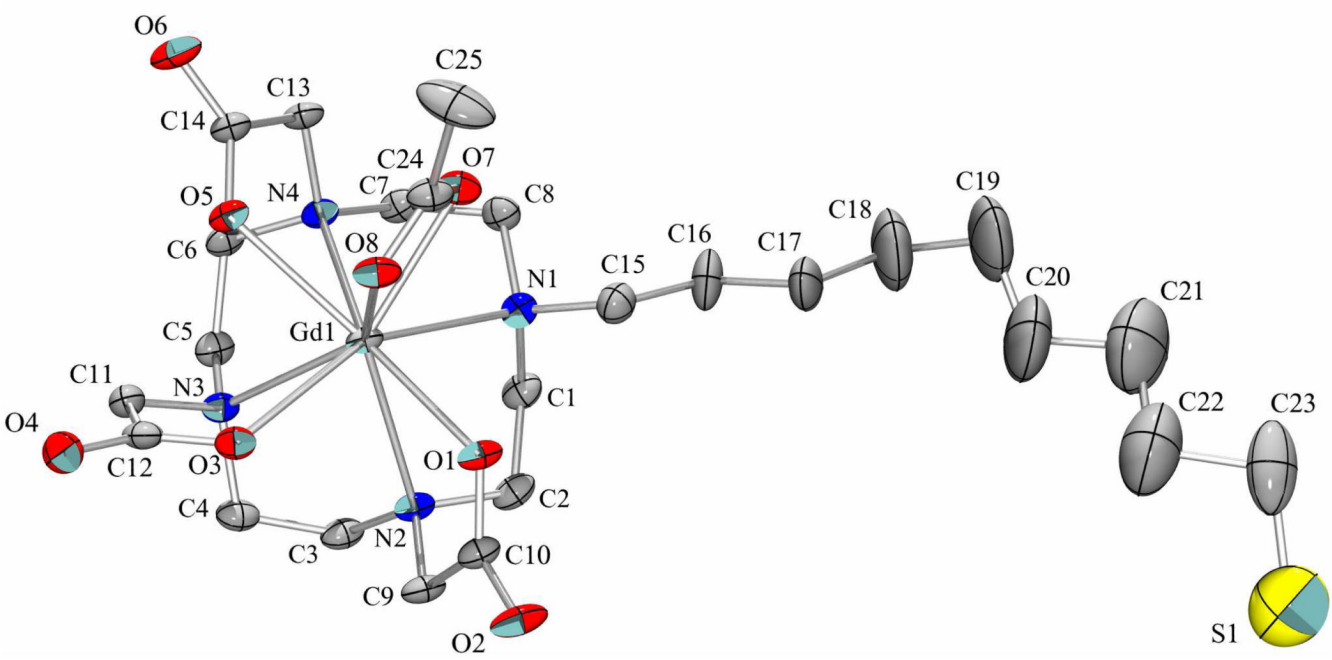

Figure 5.

The molecular structure of **4a**, with anisotropic displacement parameters at the 30% probability level. The minor disorder component, hydrogen atoms, water molecules, and the ammonium cation have been omitted for clarity.

Scheme 1.
Retrosynthetic Analysis of Ln-DO3A Conjugates **3–5**.

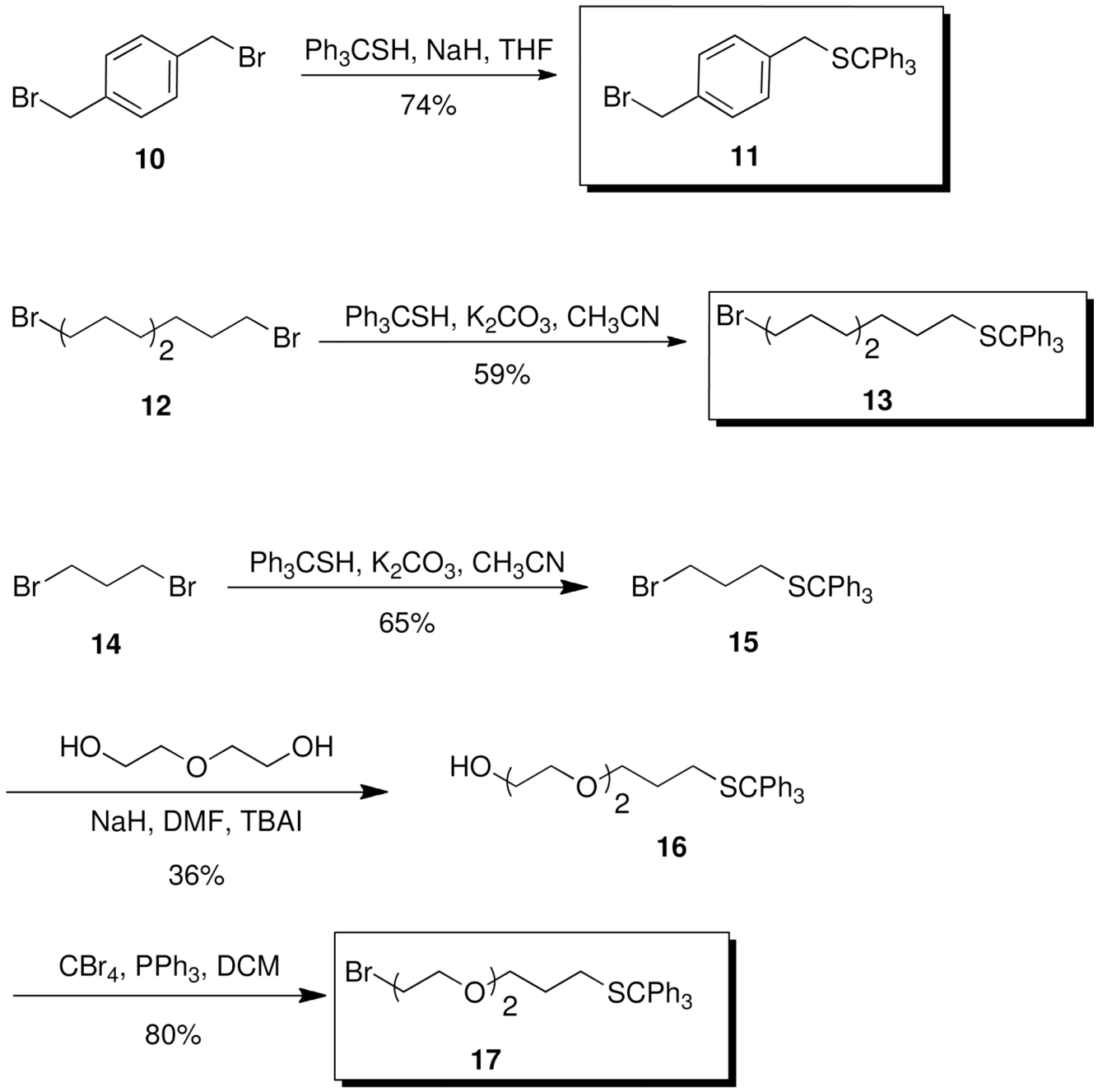

Scheme 2.
Synthesis of Bromides **11, 13**, and **17**.

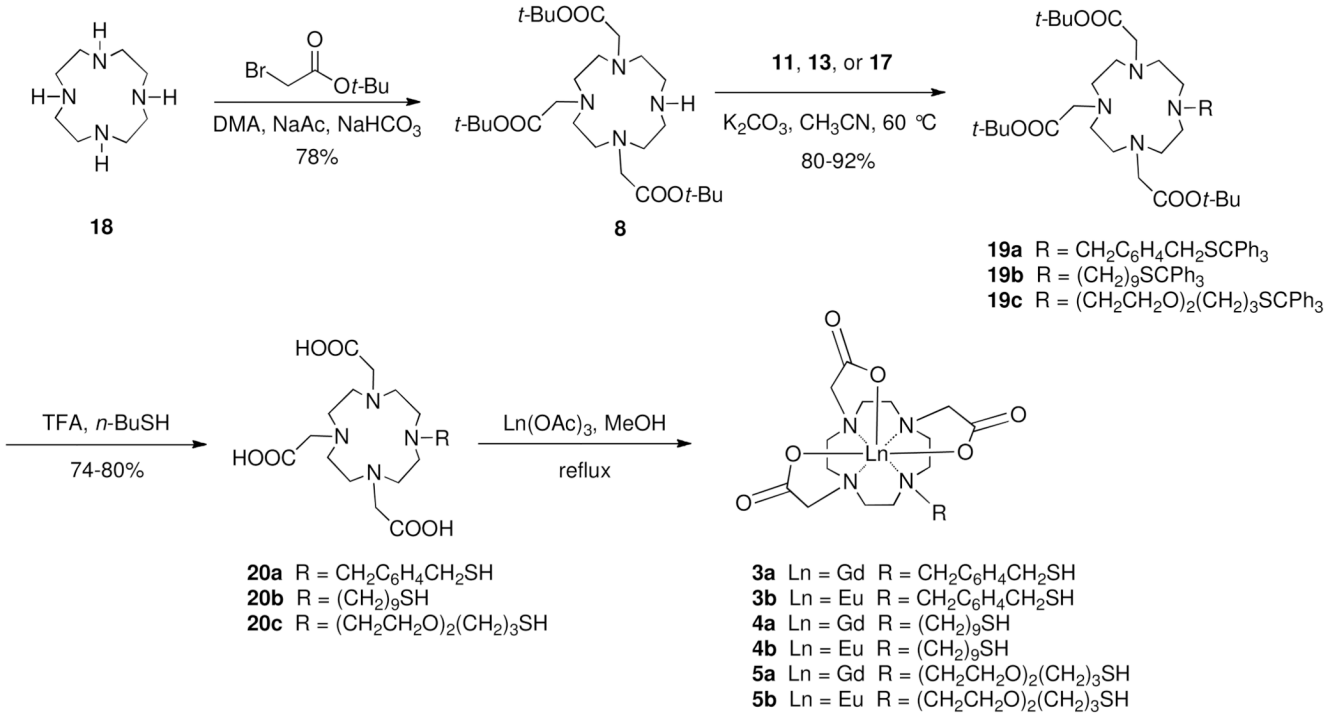

Scheme 3.
Synthesis of Gd-DO3A Complexes **3a–5a** and and Eu-DO3A Complexes **3b–5b**.

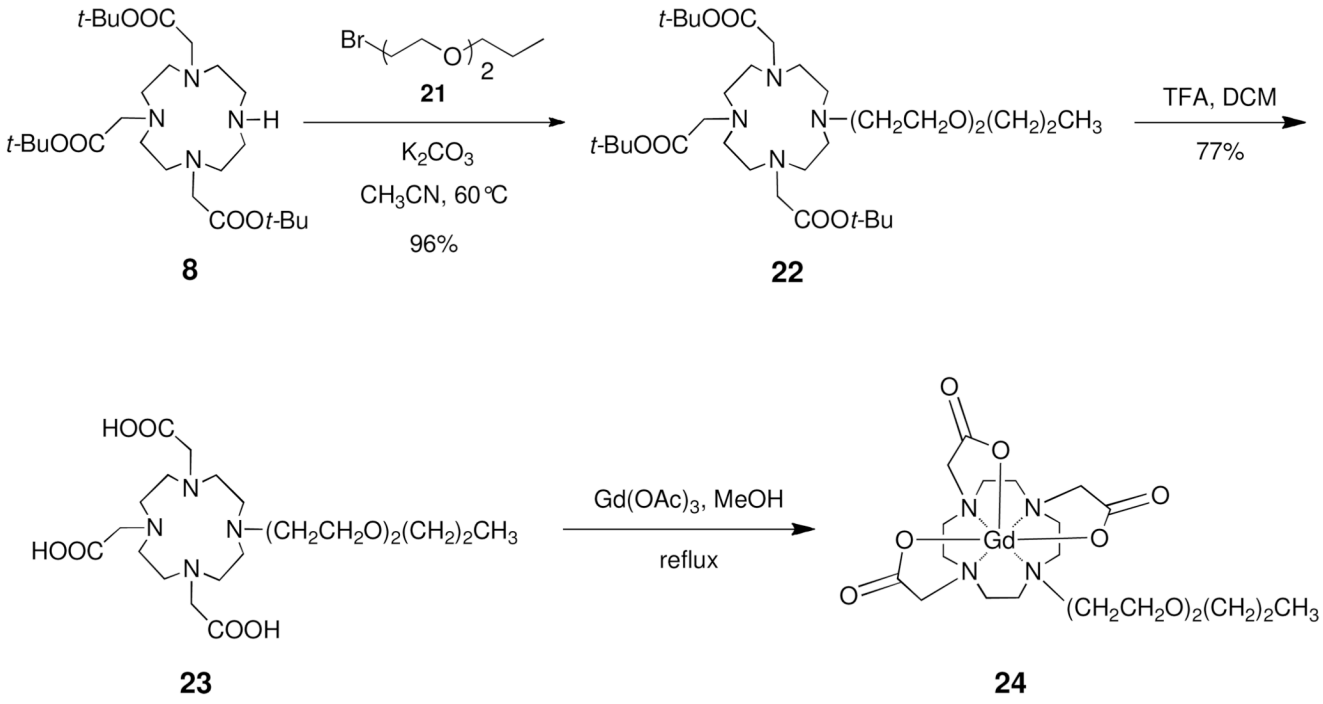

Scheme 4.
Synthesis of Gd-DO3A Complex **24**.

Table 1

Binding of Compounds **1, 2, 3a–5a**, and **24** to Human Serum Albumin.

Compound	Calculated Interaction Energy (kcal/mol)		Measured K_A[c] (mM^{-1})	Calculated Distance of Water from Gd in the	
	Covalent Complex[a]	Non-covalent Complex[b]		Presence of HSA	Absence of HSA
1[d]	−290	−210	5.0 ± 1.5	2.76 Å	2.71 Å 2.75 Å
2[d]	−510	−496	64 ± 16	2.71 Å	2.65 Å 2.72 Å
3a	−410	−366	mb[e]	2.54 Å	2.67 Å 2.89 Å
4a	−471	−404	mb[e]	2.75 Å	2.73 Å 2.74 Å
5a	−453	−413	22 ± 1.4	2.75 Å	2.73 Å 2.74 Å
24	na[f]	−406	~0	nc[g]	nc[g]

[a] Includes a disulfide bond between the compound thiol and Cys34-SH.

[b] Without a disulfide bond between the compound thiol and Cys34-SH.

[c] Measured at 37°C.

[d] Results taken from reference 31.

[e] Results suggest this compound binds to multiple sites on HSA; see text for explanation.

[f] Not applicable.

[g] Not calculated.

Table 2

Competitive Binding Study for Compounds **1**, **2**, and **5a**.[a]

Compound	Inhibitor	Inhibitor Concentration (mM)			
		0.0	0.5	1.0	2.0
			K_A (mM^{-1})		
1	homocysteine	5.0 ± 1.5	2.0 ± 0.12	1.5 ± 0.2	0.87 ± 0.05
2	homocysteine	64 ± 16	17 ± 2.2	6.1 ± 0.54	3.6 ± 0.23
5a	homocysteine	22 ± 1.4	11 ± 3.4	6.6 ± 2.7	3.4 ± 0.84
5a	**5b**	22 ± 1.4	6.2 ± 1.2	3.0 ± 0.91	~ 0

[a] Measured at 37°C.

Table 3

Relaxivities of Compounds **1**, **2**, and **3a–5a**.[a]

Compound	$r_{1,free}$ (1/mM•s)	$r_{1,bound}$ (1/mM•s)
1	3.86 ± 0.44	4.54 ± 0.14
2	3.23 ± 0.33	4.74 ± 0.32
3a	2.37 ± 0.18	1.54 ± 0.15
4a	2.27 ± 0.37	3.28 ± 0.17
5a	2.18 ± 0.58	3.15 ± 0.51

[a]Measured at 37°C and 7 Tesla.